Inorg. Chem. **2006**, *45*, 7903–7914

Coordination Chemistry of Amine Bis(phenolate) Cobalt(II), Nickel(II), and Copper(II) Complexes

Laura Rodríguez, Elena Labisbal, Antonio Sousa-Pedrares, José Arturo García-Vázquez, Jaime Romero, María Luz Durán, José A. Real,† and Antonio Sousa*

Departamento de Química Inorgánica, Universidad de Santiago de Compostela, 15782 Santiago de Compostela, Spain

Received February 15, 2006

Cobalt(II), nickel(II), and copper(II) (**1**, **2**, and **3**) complexes of the dianionic form of the bis(phenolate) ligand *N*,*N*-bis(3,4-dimethyl-2-hydroxybenzyl)-*N*′,*N*′-dimethylethylenediamine (H_2L) have been synthesized by electrochemical oxidation of the appropriate metal in an acetonitrile solution of the ligand. When copper is used as the anode, the addition of 1,10-phenanthroline to the electrolytic phase gave rise to a different compound $[CuL]_2 \cdot 2CH_3CN$ (**4**). The compounds $[CoL]_2 \cdot 2CH_3CN$ (**1**), $[Ni_2L_2(H_2O)] \cdot H_2O$ (**2**), $[CuL]_2 \cdot 3H_2O$ (**3**), and $[CuL]_2 \cdot 2CH_3CN$ (**4**) were characterized by microanalysis, IR, electronic spectroscopy, FAB mass spectrometry, magnetic measurements and by single-crystal X-ray diffraction. The crystal structures show that the complexes have a dinuclear structure. In compounds **1**, **3**, and **4**, two metal ions are coordinated by the two amine nitrogens and the two phenol oxygen atoms of a deprotonated pendant phenol ligand, with one phenolic oxygen atom from ligand acting as a bridge. In compounds **1** and **3**, each metal center has a geometry that is closest to trigonal bipyramidal. Magnetic susceptibility data for both compounds show an antiferromagnetic coupling with $2J = -15$ cm^{-1} for the cobalt(II) complex and a strong antiferromagnetic coupling with $2J = -654$ cm^{-1} for the copper(II) complex. However, in **4** the geometry around the metal is closer to square pyramidal and the compound shows a lower antiferromagnetic coupling ($2J = -90$ cm^{-1}) than in **3**. The nickel atoms in the dimeric compound **2** are hexacoordinate. The NiN_2O_4 chromophore has a highly distorted octahedral geometry. In this structure, a dianionic ligand binds to one nickel through the two amine nitrogen atoms and the two oxygen atoms and to an adjacent nickel via one of these oxygen atoms. The nickel atoms are linked through a triple oxygen bridge involving two phenolic oxygens, each from a different ligand, and an oxygen atom from a water molecule. The two nickel ions in **2** are ferromagnetically coupled with $2J = 19.8$ cm^{-1}.

Introduction

The chemistry of transition metal complexes of chelating alkoxide and aryl-oxide ligands is a subject of growing interest. One of the reasons for this interest is the development of novel catalytic systems for the polymerization of α-olefins.[1] A substantial amount of work has been performed on Group IV and Group V metals with monodentate phenolate[2,3] and chelating phenolate[4−6] ligands. Recently, dianionic amine bis(phenolate) ligands were used as an approach to increase the hydrophobic nature of the coordinating ligands.[7] However, the use of chelating phenolates in other transition-metal groups is still rare.[8,9] In addition, interest in the structure and reactivity of transition metal complexes with this type of ligand is related, in part, to the

* To whom correspondence should be addressed. Phone: +34-981563100, ext 14245. Fax: +34-981597525. E-mail: qiansoal@usc.es.
† Institut de Ciéncia Molecular, Universitat de València, Doctor Moliner 50, 46100 Burjassot, València, Spain.

(1) Britovsek, G. J. P.; Gibson, V. C.; Wass, D. F. *Angew. Chem., Int. Ed.* **1999**, *38*, 428−447.
(2) Van der Linden, A.; Schaverien, C. J.; Meijboom, N.; Ganter, C.; Orpen, A. G. *J. Am. Chem. Soc.* **1995**, *117*, 3008−3021.
(3) (a) Fokken, S.; Spaniol, T. P.; Kang, H.-C.; Massa, W.; Okuda, J. *Organometallics* **1996**, *15*, 5069−5072. (b) Fokken, S.; Spaniol, T. P.; Okuda, J.; Sernetz, F. G.; Mülhaupt, R. *Organometallics* **1997**, *16*, 4240−4242.
(4) Tshuva, E. Y.; Versano, M.; Goldberg, I.; Kol, M.; Weitman, H.; Goldschmidt, Z. *Inorg. Chem. Commun.* **1999**, *2*, 371−373.
(5) (a) Rothwell, I. P. *Acc. Chem. Res.* **1988**, *21*, 153−159. (b) Schweiger, S. W.; Tillison, D. L.; Thorn, M. G.; Fanwick, P. E.; Rothwell, I. P. *J. Chem. Soc., Dalton Trans.* **2001**, 2401−2408.
(6) Wigley, D. E.; Gray, S. D. *Comprehensive Organometallic Chemistry, III*; Abel, E. W., Stone, F. G. A., Wilkinson, G., Eds.; Pergamon Press: Oxford, England, 1995; Vol. 5, pp 57−153.
(7) Caulfield, M. J.; Russo, T.; Solomon, D. H. *Aust. J. Chem.* **2000**, *53*, 545−549.

10.1021/ic0602594 CCC: $33.50
Published on Web 08/23/2006

fact that they can be used as mimetic small molecular models for the active sites of several redox and hydrolytic enzymes.[10,11] In particular, in the case of nickel, Yamaguchi et al.[12] reported a carboxylate-bridged dinuclear Ni(II) model complex that catalyzes the ethanolysis of urea to ethyl carbamate. In this system, the geometry of one of the nickel sites is pseudotetrahedral while the other nickel site is approximately trigonal pyramidal. In the case of copper, the rational design of ligands that can induce asymmetry in binuclear copper complexes is a suitable strategy for better understanding the mechanisms of copper-containing enzymes, such as tyrosinase or catechol oxidase.[13] The former is a mono-oxygenase that uses dioxygen in the hydroxylation of monophenols to diphenols, further acting as a two-electron oxidase in the oxidation of *o*-diphenols to *o*-quinones. The latter system catalyzes the oxidation of catechols to quinones without acting on tyrosine.[14]

The ability of aryl-oxide-functionalized ligands to efficiently facilitate the magnetic coupling between two paramagnetic metal ions represents another source of interest in the realm of molecular magnetism.[15,16]

Indeed, dinucleating ligands that contain a potentially bridging phenoxo oxygen and nitrogen donor sets have been widely used in the synthesis of dinuclear complexes of copper,[17] manganese,[18] cobalt,[19] iron,[20] and zinc.[19] As in hydroxo- and alkoxo-bridged metal complexes, the nature of the magnetic interactions in phenoxo-bridged metal systems is primarily determined by the M−O−M angle and the M···M separation.[21,22]

As part of our research in this area, we report here the preparation, structure determination, and properties of dinuclear nickel, copper, and cobalt complexes of the sterically hindered tripodal ligand *N*,*N*-bis(3,4-dimethyl-2-hydroxybenzyl)-*N*′,*N*′-dimethylethylenediamine [H_2L] (Figure 1). This ligand contains two phenol pendant groups and was obtained by a Mannich reaction between a disubstituted phenol, formaldehyde, and *N*,*N*-dimethylethylenediamine.

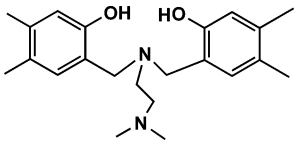

Figure 1.

Experimental Section

General Considerations. All solvents and 3,4-dimethylphenol, *N*,*N*-dimethylethylenediamine, and 37% aq formaldehyde were commercial products (Aldrich) and were used as supplied. Cobalt, nickel, and copper (Ega Chemie) were used as 2 × 2 cm^2 plates.

Microanalyses were performed using a Perkin-Elmer 240B microanalyzer. IR spectra were recorded on a Perkin-Elmer 1330 spectrophotometer. Diffuse reflectance spectra were recorded on a Shimadzu UV-3101PC spectrophotometer. ^1H and ^{13}C NMR spectra were recorded in deuterated $CDCl_3$ with a Bruker WM 350 MHz spectrometer. The FAB mass spectra of the complexes were recorded on a Micromass Autospec instrument and the electrospray mass spectra on a Hewlett-Packard 1100 spectrometer. Variable-temperature magnetic susceptibility measurements were carried out using microcrystalline samples (20−60 mg) of compounds **1**−**4**, using a Quantum Design MPMS2 SQUID susceptometer equipped with a 5.5 T magnet, operating at 0.1−0.5 T and at temperatures from 300 to 1.8 K. The susceptometer was calibrated with $(NH_4)_2Mn(SO_4)_2 \cdot 12H_2O$. Experimental susceptibilities were corrected for diamagnetism of the constituent atoms by the use of Pascal's constants.

Ligand Synthesis. The ligand H_2L was prepared by condensation between *N*,*N*-dimethylethylenediamine (2.7 mL, 25 mmol), formaldehyde 37% (3.7 mL, 50 mmol), and 3,4-dimethylphenol (6.10 g, 50 mmol) in methanol (250 mL). The solution was heated under reflux for 5 h and then cooled (4 °C). The resulting white precipitate was filtered off and recrystallized (dichloromethane/methanol) to give white crystals of H_2L. Anal. Found (Calcd) for $C_{22}H_{32}N_2O_2$: C, 73.99 (74.12); H, 9.10 (9.05), N, 7.77 (7.86)%. ^1H NMR ($CDCl_3$, ppm) 9.6 (s br, 2H, OH), 6.75 (s, 2H, phenyl), and 6.60 (s, 2H, phenyl), 3.55 (s, 4H, CH_2), 2.57 (m, 4H, CH_2), 2.30 (s, 6H, CH_3), 2.16 (s, 6H, CH_3) and 2.13 (s, 6H, CH_3). ^{13}C NMR ($CDCl_3$, ppm) 155 (C−OH), 137.5, 131.1, 126.6, 119.5 and 118.0 (phenyl), 60.8, 56.3, 55.3 and 49.0 (N−CH_2), 44.8 (N−CH_3), 19.6 and 18.0 (N−CH_3). IR (KBr, cm^{-1}): 465(w), 538 (vw), 709(vw), 732(vw), 778-(m), 804(m), 829(m), 863(m), 889(m), 931(m), 981(m), 1001(m), 1023(m), 1106(s), 1124(w), 1295(m), 1238 (m), 1294(vs), 1332-(s), 1365(m), 1468(s), 1503(s), 1573(vs), 1628(w), 2827(w), 2854 (m), 2922(w), 2941(vw), 2966(w), 3400(vbr). EI MS; *m*/*z*: 356 (M^+, 100%).

(8) Castellano, B.; Solari, E.; Florián, C.; Re, N.; Chiesi-Villa, A.; Rizzoli, C. *Chem. Eur. J.* **1999**, *5*, 722−737.
(9) Michalczyk, L.; de Gala, S.; Bruno, J. W. *Organometallics* **2001**, *20*, 5547−5556.
(10) Kolodziej, A. F. In *Progress in Inorganic Chemistry*; Karlin, K. D., Ed.; Wiley: New York, 1994; pp 494−597.
(11) (a) Kovac, J. A. In *Advances in Inorganic Biochemistry*; Eichorn, G. L., Marzilli, L. G., Eds.; Prentice Hall; Englewood Cliffs, NJ, 1993; p 9. (b) Commack, R.; Hall, D. O.; Rao, K. K. In *Microbial gas metabolism mechanistic, metabolic and biotechnological aspects*; Poole, R. K., Dow, C. S., Eds.; Academic Press: London; 1985; p 209. (c) Kubas, G. *Acc. Chem. Res.* **1988**, *21*, 120−128.
(12) Yamaguchi, K.; Koshino, S.; Akagi, F.; Suzuki, M.; Uehara, A.; Suzuki, S. *J. Am. Chem. Soc.* **1997**, *119*, 5752−5753.
(13) Zippel, F.; Ahlers, F.; Werner, R.; Haase, W.; Nolting, H.-F.; Krebs, B. *Inorg. Chem.* **1996**, *35*, 3409−3419.
(14) Tremolières, M.; Bieth, J. G. *Phytochemistry* **1984**, *23*, 501−505.
(15) Reed, C. A.; Orosz, R. D. *Spin Coupling Concepts in Bioinorganic Chemistry*; O'Connor, C. J., Ed.; World Scientific: Singapore, 1993; pp 351−393. Gatteschi, R.; Sessoli, A. Cornia, *Comprehensive Coordination Chemistry*, *II*; Elsevier: New York, 2004; Vol. 7, pp 779−813.
(16) Melnik, M.; Kabesová, M.; Koman, M.; Macáskova, L.; Garaj, J.; Holloway, C. E.; Valent, *J. Coord. Chem.* **1998**, *45*, 147−359. Thompson, L. K., Ed.; *Coord. Chem. Rev.* **2005**, *249*, 2549−2729.
(17) (a) Karlin, K. D.; Cruse, R. W.; Gultneh, Y.; Hayes, J. C.; Zubieta, J. *J. Am. Chem. Soc.* **1984**, *106*, 3372−3374. (b) Sorrel, T. N.; Garrity, M. L. *Inorg. Chem.* **1991**, *30*, 210−215.
(18) Diril, H.; Chang, H.-R.; Zhang, X.; Larasen, S. K.; Potenza, J. A.; Pierpont, C. G.; Schugar, H. J.; Isied, S. S.; Hendrickson, D. N. *J. Am. Chem. Soc.* **1987**, *109*, 6207−6208.
(19) (a)Suzuki, M.; Kanatomi, H.; Murase, I. *Chem. Lett*. **1981**, 1745−1748. (b) Suzuki, M.; Ueda, I.; Kanatomi, H.; Murase, I. *Chem. Lett*. **1983**, 185−188.
(20) (a) Nie, H.; Aubin, S. M. J.; Mashuta, M. S.; Wu, C.-H.; Richardson, J. F.; Hendrickson, D. N.; Buchanan, R. M. *Inorg. Chem.* **1995**, *34*, 2382−2388. (b) Uhlenbrock, S.; Krebs, B. *Angew. Chem., Int. Ed. Engl.* **1992**, *31*, 1647−1648.
(21) (a) Crawford, V. H.; Richardson, H. W. Wasson, J. R.; Hodgson, D. J.; Hatfield, W. E. *Inorg. Chem.* **1976**, *15*, 2107−2110. (b) Hodgson, D. J. *Prog. Inorg. Chem.* **1975**, *19*, 173−241. (c) Asokan, A.; Varghese, B.; Manoharan, P. T. *Inorg. Chem.* **1999**, *38*, 4393−4399. (d) Bertoncello, K.; Fallon, G. D.; Hodgkin, J. H.; Murray, K. S. *Inorg. Chem.* **1988**, *27*, 4750−4758. (e) Karlin, K. D., Farooq, A.; Hayes, J. C.; Cohen, B. I.; Rowe, T. M.; Sinn, E.; Zubieta, J. *Inorg. Chem.* **1987**, *26*, 1271−1280.
(22) Gupta, R.; Mukherjee, S.; Mukherjee, R. *J. Chem. Soc., Dalton Trans*. **1999**, 4025−4030.

Scheme 1

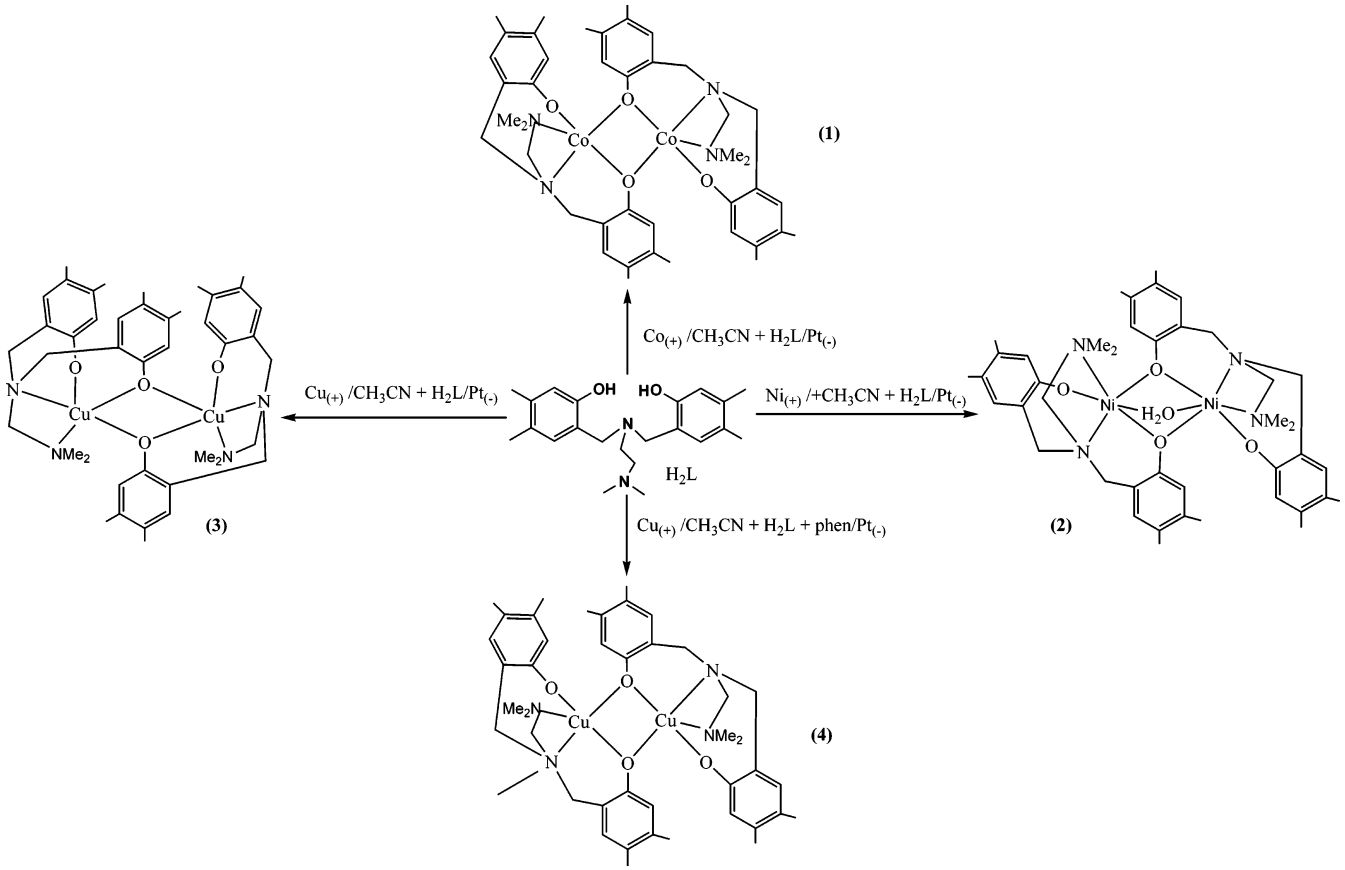

Electrochemical Synthesis of Metal Complexes. The complexes were obtained using an electrochemical procedure (Scheme 1). The cell can be summarized as $Pt_{(-)}|H_2L + MeCN|M_{(+)}$. A platinum wire was used as the cathode and a metal plate as the anode. Tetramethylammonium perchlorate (10 mg) was added to the solution. Applied voltages of 10−20 V allowed sufficient current flow for smooth dissolution of the metal.

Synthesis of $[CoL]_2 \cdot 2CH_3CN$ (1). A solution of H_2L (0.03 g, 0.09 mmol) in acetonitrile (70 mL) containing about 10 mg of tetramethylammonium perchlorate as supporting electrolyte was electrolyzed for 1 h with a current of 5 mA. A platinum wire was used as the cathode and a cobalt plate as the anode; $E_f = 0.50$ mol F^{-1}. A small quantity of an insoluble unidentified product was filtrered off. The mother liquor was left to stand for 1 week. Slow evaporation of the solution yielded small dark pink crystals of $[CoL]_2 \cdot 2CH_3CN$ that were suitable for X-ray diffraction. Anal. Found (Calcd) for $C_{48}H_{66}Co_2N_6O_4$: C, 63.54 (63.43); H, 7.14 (7.31); N, 9.12 (9.25). IR (KBr, cm^{-1}): 450(m), 550(m), 636(m), 723(m), 753(s), 772(m), 820(m), 841(m), 878(s), 938(m), 980(w), 1001-(m), 1020(m), 1102(vs), 1174(w), 1211(m), 1290(vs), 1308(s), 1361(m), 1455(s), 1488(vs), 1549, (w), 1612(m), 2843(w), 2922-(w), 2970(w), 3400(br), 3615(br).

Synthesis of $[Ni_2L_2(H_2O)] \cdot H_2O$ (2). In an experiment similar to that described above, a solution of H_2L (0.03 g, 0.09 mmol) in acetonitrile (70 mL) was electrolyzed for 1 h with a current of 5 mA. Green crystals of $[Ni_2L_2(H_2O)] \cdot H_2O$ were obtained using nickel as the anode, $E_f = 0.50$ mol F^{-1}. Anal. Found (Calcd) for $C_{44}H_{64}N_4Ni_2O_6$: C, 60.91 (61.28); H, 7.45 (7.48); N, 6.67 (6.50). IR (KBr, cm^{-1}): 440(w), 525(w), 570(w), 622 (m), 640(w), 710(w). 755-(m), 770(m), 855(w), 875(m), 935(m), 950(m), 1000(w), 1023(m), 1096(vs), 1179(vw), 1210(vw), 1260(w), 1307(m), 1330(m), 1407-(m), 1458(s), 1489(s), 1550(w), 1610(s), 2837(w), 2857(m br), 2923(w), 2993(m,br), 3500(br).

Synthesis of $[CuL]_2 \cdot 3H_2O$ (3). An orange solid of empirical formula $[Cu_2L_2] \cdot 3H_2O$ was obtained by the same method, using copper as the anode, $E_f = 1.00$ mol F^{-1}. Recrystallization of the brown solid from acetonitrile yielded orange crystals of $[CuL]_2 \cdot 3H_2O$. Anal. Found (Calcd) for $C_{44}H_{66}Cu_2N_4O_7$: C, 59.61 (59.37); H, 7.45 (7.47); N, 6.60 (6.29). IR (KBr, cm^{-1}): 510(w), 560(w), 607(m), 637(w), 723(m), 754(s), 772(m), 820(w), 857(m), 893-(m), 933(m), 972(m), 1000(w), 1019(m), 1100(vs), 1173(w), 1211-(m), 1293(s), 1314(vs), 1331(s), 1361(m), 1407(m), 1455(s), 1495(vs), 1550(w), 1607(s), 1655(w), 2792(w), 2842(w), 2862(w), 2892(w), 2923(w), 3600(m).

Synthesis of $[CuL]_2 \cdot 2CH_3CN$ (4). An solution of H_2L (0.03 g, 0.09 mmol) and phen (0.0184 g, 0.09 mmol) in acetonitrile (70 mL) was electrolyzed for 1 h (5 mA 15 V) using a copper plate as the anode, $E_f = 0.97$ mol F^{-1}. Dark brown crystals were obtained by slow evaporation of the resulting solution. Anal. Found (Calcd) for $C_{48}H_{66}Cu_2N_6O_4$: C, 62.64 (62.79); H, 7.45 (7.25); N, 9.06 (9.15). IR (KBr, cm^{-1}): 629(w), 813(m), 821(w), 845(m), 857-(m), 878(m), 892(m), 933(w), 972 (m), 998(m), 1019(m), 1029-(w), 1102(vs), 1172(w), 1211(m), 1266(w), 1294 (s), 1318(vs), 1358(w), 1370(w), 1408(m), 1455(s), 1494(vs), 1549(w), 1611(s), 1638(w), 2251(w), 2792(w), 2841(w), 2857(w), 2890(w), 2918-(w).

X-ray Crystallographic Studies. Intensity data sets for compounds **1** and **2** were collected using a Smart-CCD-1000 Bruker diffractometer (Mo Kα radiation, $\lambda = 0.71073$ Å) equipped with a graphite monochromator. Intensity data for compound **3** were collected using a CAD4 Enraf Nonius diffractometer (Mo Kα radiation, $\lambda = 0.71073$ Å) equipped with a graphite monochromator.

Table 1. Summary of Crystallographic Data and Refinement

	1	2	3	4
empirical formula	$C_{48}H_{66}Co_2N_6O_4$	$C_{44}H_{64}N_4Ni_2O_6$	$C_{44}H_{66}Cu_2N_4O_7$	$C_{48}H_{66}Cu_2N_6O_4$
fw	908.93	862.41	890.09	918.15
cryst size (mm^3)	0.40 × 0.39 × 0.10	0.26 × 0.26 × 0.07	0.40 × 0.20 × 0.08	0.28 × 0.22 × 0.06
temp (K)	293(2) K	293(2) K	293(2) K	293(2) K
cryst syst	monoclinic	orthorhombic	monoclinic	triclinic
space group	*C*2/*c*	*Pbcn*	*C*2/*c*	$P\bar{1}$
a (Å)	23.057(6)	30.734(5)	20.434(13)	9.0313(15)
b (Å)	11.645(3)	20.182(3)	8.349(2)	11.0953(18)
c (Å)	17.383(4)	21.840(3)	27.166(8)	12.8729(19)
α (deg)	90	90	90	80.9300(10)
β (deg)	95.410(6)	90	106.72(4)	73.8700(10)
γ (deg)	90	90	90	72.9800(10)
V ($Å^3$)	4646.6(18)	13547(3)	4439(3)	1180.8(3)
Z	4	12	4	1
F(000)	1928	5520	1888	486
abs coeff (mm^{-1})	0.763	0.882	1.010	1.487
wavelength (Å)	0.71073	0.71073	0.71073	1.54180
d_{calcd} (g/cm^3)	1.299	1.269	1.332	1.291
reflns collected	4791	39 888	3240	5087
unique reflns [*R*int]	4791 [*R*(int) = 0.0000]	8247 [*R*(int) = 0.1360]	3161 [*R*(int) = 0.1896]	4830 [*R*(int) = 0.0112]
data/restraints/params	4791/0/272	8247/2/782	3161/3/270	4830/0/272
θ range for data collection	1.77−26.48°	1.86−21.97°	2.65−23.37°	3.59−74.96°
GOF on F^2	1.081	0.930	0.941	1.063
final *R* indices [$I > 2\sigma(I)$]	R1 = 0.0342 wR2 = 0.0813	R1 = 0.0517 wR2 = 0.1123	R1 = 0.0633 wR2 = 0.0971	R1 = 0.0378, wR2 = 0.1118
R indices (all data)	R1 = 0.0582 wR2 = 0.0981	R1 = 0.1777 wR2 = 0.1571	R1 = 0.3205 wR2 = 0.1357	R1 = 0.0440 wR2 = 0.1164
largest diff. peak and hole e.$Å^{-3}$	0.309 and −0.437	0.728 and −0.415	0.453 and −0.694	0.446 and −0.42

Intensity data for compound **4** were collected using a MACH3 Enraf Nonius diffractometer (Cu Kα radiation; $\lambda = 1.54180$ Å) equipped with a graphite monochromator. All crystals were studied at 293 K. The *ω* scan technique was employed to measure intensities in all crystals. Decomposition of the crystals was not detected during data collection. The intensities of all data sets were corrected for Lorentz and polarization effects. Absorption effects in compounds **1** and **2** were corrected using the program SADABS;[23] absorption in **3** and **4** was corrected using semiempirical *ψ* scans. The crystal structures of all compounds were solved by direct methods. Crystallographic programs used for structure solution and refinement were those in SHELX97.[24] Scattering factors were those provided with the SHELX program system. Missing atoms were located in the difference Fourier map and included in subsequent refinement cycles. The structures were refined by full-matrix least-squares refinement on F^2. Hydrogen atoms not involved in hydrogen bonding were placed geometrically and refined using a riding model with U_{iso} constrained at 1.2 (for nonmethyl groups) and 1.5 (for methyl groups) times U_{eq} of the carrier C atom. For all structures, non-hydrogen atoms were anisotropically refined and in the last cycles of refinement a weighting scheme was used, with weights calculated using the following formula $w = 1/[\sigma^2(F_o^2) + (aP)^2 + bP]$, where $P = (F_o^2 + 2F_c^2)/3$. Compounds **2** and **3** were poor diffractor crystals, so their maximum *θ* values were rather low.

Pertinent details of the data collections and structure refinements are summarized in Table 1. Further details regarding the data collections, structure solutions, and refinements are included in the Supporting Information. ORTEP3 drawings[25] with the numbering scheme used are shown in Figures 2, 3, 5, and 7.

Crystallographic data (excluding structure factors) for the structures reported in this paper have been deposited with the Cambridge Crystallographic Data Centre as supplementary publication no. CCDC 297244-297247 [**1**, **2**, **3**, and **4**]. Copies of the data can be obtained free of charge on application to CCDC, 12 Union Road, Cambridge CB21EZ, UK (fax: (+44) 1223-336-033; e-mail: deposit@ccdc.cam.ac.uk).

Results and Discussion

Ligand Synthesis. The ligand H_2L was synthesized by the one-pot Mannich condensation between *N*,*N*-dimethylethylenediamine, formaldehyde, and 3,4-dimethylphenol. The resulting pale white powder was characterized by elemental analysis and IR, ^1H NMR, and ^{13}C NMR spectroscopy.

Synthesis of the Complexes. A series of neutral complexes were obtained by electrochemical oxidation of the corresponding metal anode in the presence of the ligand.[26] For cobalt and nickel, the electrochemical efficiency of the cell was close to 0.50 mol F^{-1}, which is compatible with the following reaction scheme:

$$\text{Cathode: } H_2L + 2e^- \rightarrow H_2(g) + L^{2-}$$

$$\text{Anode: } L^{2-} + M \rightarrow ML + 2e^-$$

$$M = \text{Co and Ni}$$

An E_f value close to 1 mol F^{-1} was found in the case of the copper complex, which indicates that the anodic oxidation leads initially to a Cu(I) compound. However, the analytical data show that the complex is [CuL]. This observation suggests that the ligand oxidizes the Cu(I) to Cu(II) in solution as soon as it is formed

$$\text{Cathode: } H_2L + e^- \rightarrow 1/2H_2(g) + HL^-$$

$$\text{Anode: } Cu \rightarrow Cu^+ + e^-$$

$$HL^- + Cu^+ \rightarrow [CuL]\ (\mathbf{3}) + 1/2H_2(g)$$

(23) Sheldrick, G. M. *SADABS: Program for absorption correction using area detector data*; University of Göttingen: Göttingen, Germany, 1996.
(24) Sheldrick, G. M. *SHELX97* [Includes *SHELXS97*, *SHELXL97*, *CIFTAB*]− *Programs for Crystal Structure Analysis* (Release 97-2); Institüt für Anorganische Chemie der Universität: Göttingen, Germany, 1998.
(25) Farrugia, L. J. *ORTEP3 for Windows*; *J. Appl. Crystallogr.* **1997**, *30*, 565.

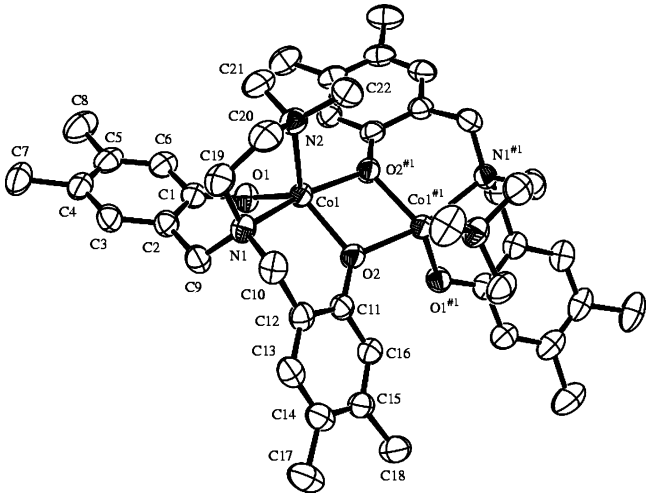

Figure 2. ORTEP diagram of the molecular structure of **1** with 50% thermal ellipsoid probability.

This behavior has been observed previously in the synthesis of other copper complexes by an electrochemical procedure.[27]

The electrochemical oxidation of copper in a solution of the ligand H_2L and an equimolecular amount of 1,10-phenanthroline in acetonitrile gave the homoleptic complex **4**, showing that the coligand had not been incorporated into the metal coordination sphere. Compound **4** prepared in this way is isomeric to complex **3**, the synthesis of which was carried out in the absence of coligands. Once again, an E_f value of 1 suggests that the mechanism for the formation of compound **4** is similar to that outlined for **3**.

This synthetic procedure allows the synthesis of neutral $[ML]_2$ complexes with high purity and in very good yield.

Elemental analyses show that metal ions react with the ligand in a 1:1 molar ratio to afford complexes of the bis-(deprotonated) ligand L^{2-}. These neutral complexes are either insoluble or sparingly soluble in water and common organic solvents, but they are soluble in polar coordinating organic solvents such as DMSO, DMF, and pyridine. The compounds appear to be stable both in the solid state and in solution, and they all melt above 300 °C.

Description of Structures. The complexes **1**, **2**, **3**, and **4** were studied by X-ray diffraction. The crystal parameters, experimental details for data collection, and bond distances and angles for all these compounds are provided as Supporting Information.

Structure of $[CoL]_2 \cdot 2CH_3CN$. The molecular structure of $[CoL]_2$ is shown in Figure 2 together with the labeling scheme used. Selected bond distances and angles with estimated standard deviations are listed in Table 2.

The structure consists of $[CoL]_2$ dimers. Each cobalt atom is coordinated by the two amine nitrogen and the two phenol oxygen atoms of a deprotonated pendant phenol ligand and by another phenol oxygen atom from another similar fragment. The four-membered ring formed by the two cobalt atoms and the two oxygen atoms of the bridge is essentially planar, and none of the atoms deviates from the least-squares plane by more than 0.048 Å. However, the bridge is slightly asymmetric, [Co(1)−O(2)] 1.9900 (15) Å and [Co(1)−O(2)*] 2.0678(16) Å and the two cobalt(II) centers are separated by 3.1547(8) Å, which is similar to the situation found in other phenoxo-bridged dinuclear cobalt(II) complexes.[28,29]

Table 2. Selected Bond Lengths [Å] and Angles [deg] for **1**[a]

Co(1)−O(1)	1.9289(16)	Co(1)−O(2)	1.9900(15)
Co(1)−O(2)#1	2.0678(16)	Co(1)−N(2)	2.156(2)
Co(1)−N(1)	2.1885(19)	Co(1)−Co(1)#1	3.1547(8)
O(1)−Co(1)−O(2)	122.03(7)	O(1)−Co(1)−O(2)#1	104.21(7)
O(2)−Co(1)−O(2)#1	77.70(7)	O(1)−Co(1)−N(2)	111.31(7)
O(2)−Co(1)−N(2)	126.34(7)	O(2)#1−Co(1)−N(2)	95.55(7)
O(1)−Co(1)−N(1)	91.08(7)	O(2)−Co(1)−N(1)	90.75(7)
O(2)#1−Co(1)−N(1)	164.15(7)	N(2)−Co(1)−N(1)	82.47(8)
Co(1)−O(2)−Co(1)#1	102.04(7)		

[a] Symmetry transformations used to generate equivalent atoms: #1 $-x+1, y, -z+1/2$.

The value of the trigonality index,[30] τ, is 0.63 [where β represents the angle N(2)−Co(1)−O(2) = 126.34(7)° and α represents O(2)*−Co(1)−N(1) = 164.15 (7)°], and this shows that the complex has a geometry closer to trigonal-bipyramidal ($\tau = 1$) than to a square-pyramidal ($\tau = 0$). The equatorial plane consists of the two phenol oxygen atoms and one of the nitrogen atoms of the tetradentate ligand. The other nitrogen atom and the bridging oxygen atom are in the apical positions. The cobalt atom deviates by 0.066 Å from the equatorial plane NO_2.

The angles around the metal atom in the equatorial plane are differ from the ideal value of 120°; N(2)−Co(1)−O(1) 111.31(7), O(1)−Co(1)−O(2) 122.03(7)°, and O(2)−Co(1)−N(2) 126.34(7)°.

Bond lengths between the Co and phenol oxygen atoms vary significantly [O(2)−Co(1) 1.9900(15), O(1)−Co(1) 1.9289(16), and O*(2)−Co(1) 2.0678(16) Å], with the shorter value corresponding to the apical oxygen phenoxy terminal atom. However, these distances do fall in the range defined by the average $Co-O_{phenoxy}$ values observed in other pentacoordinated cobalt(II) complexes [1.891(6)−2.099(4) Å].[28,29,31,32] The $Co-N_{amine}$ distances are similar [Co(1)−N(2) 2.156(2) Å and Co(1)−N(1) 2.1885(19) Å] and are close to the bond distances in other pentacoordinated cobalt complexes [2.092(4)−2.197(5) Å].[28,32,33]

The compound crystallizes with two acetonitrile solvent molecules, which do not interact with the cobalt complex in any significant manner, and there are no noteworthy intermolecular contacts.

Structure of $[Ni_2L_2(H_2O)] \cdot H_2O$. The molecular structure of the complex is shown in Figure 3 along with the atom

(26) Oldham, C.; Tuck, D. G. *J. Chem. Educ.* **1982**, *59*, 420−421.
(27) Beloso, I.; Borrás, J.; Castro, J.; García-Vázquez, J. A.; Pérez-Lourido, P.; Romero, J. Sousa, A. *Eur. J. Inorg. Chem.* **2004**, 635−645.
(28) Du, M.; An, D. L.; Guo, Y. M.; Bu, X. H. *J. Mol. Struct.* **2002**, *641*, 193−198.
(29) Furutachi, H.; Okawa, H. *Inorg. Chem.* **1997**, *36*, 3911−3918.
(30) Addison, A. W.; Rao, T. N.; Reedjik, J.; Van Rijn, J.; Vershcoor, G. C. *J. Chem. Soc., Dalton, Trans.* **1984**, 1349−1356.
(31) Kita, S.; Furutachi, H. H.; Okawa, H. *Inorg. Chem.* **1999**, *38*, 4038−4045.
(32) Cini, R. *Acta Crystallogr.* **2001**, *C57*, 1171−1173.
(33) Boca, R.; Elias, H.; Haase, W.; Huber, M.; Klement, R.; Muller, L.; Paulus, H.; Svoboda, I.; Valko, M. *Inorg. Chim. Acta* **1998**, *278*, 127−135.

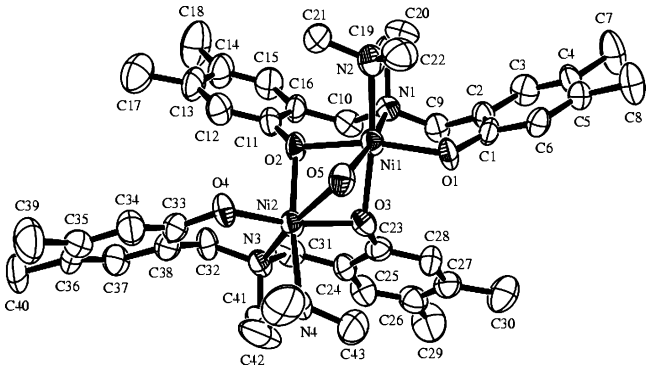

Figure 3. ORTEP diagram of the molecular structure of **2** with 50% thermal ellipsoid probability.

Table 3. Selected Bond Lengths [Å] and Angles [deg] for **2**[a]

Ni(1)−O(2)	1.983(5)	Ni(1)−O(1)	1.998(5)
Ni(1)−N(1)	2.057(7)	Ni(1)−O(3)	2.088(6)
Ni(1)−N(2)	2.157(7)	Ni(1)−O(5)	2.253(7)
Ni(1)−Ni(2)	2.9126(15)	Ni(2)−O(4)	1.972(6)
Ni(2)−O(3)	1.987(6)	Ni(2)−N(3)	2.053(7)
Ni(2)−O(2)	2.076(5)	Ni(2)−N(4)	2.163(7)
Ni(2)−O(5)	2.232(7)	Ni(3)−O(7)	1.960(6)
Ni(3)−O(6)	1.980(6)	Ni(3)−N(5)	2.068(7)
Ni(3)−O(6)#1	2.070(5)	Ni(3)−N(6)	2.153(7)
Ni(3)−O(8)	2.217(7)	Ni(3)−Ni(3)#1	2.925(2)
O(2)−Ni(1)−O(1)	166.8(2)	O(2)−Ni(1)−N(1)	94.8(3)
O(1)−Ni(1)−N(1)	95.0(3)	O(2)−Ni(1)−O(3)	78.8(2)
O(1)−Ni(1)−O(3)	90.0(2)	N(1)−Ni(1)−O(3)	106.4(3)
O(2)−Ni(1)−N(2)	95.7(3)	O(1)−Ni(1)−N(2)	93.9(3)
N(1)−Ni(1)−N(2)	85.0(3)	O(3)−Ni(1)−N(2)	167.7(3)
O(2)−Ni(1)−O(5)	77.4(3)	O(1)−Ni(1)−O(5)	92.9(3)
N(1)−Ni(1)−O(5)	172.1(3)	O(3)−Ni(1)−O(5)	73.7(2)
N(2)−Ni(1)−O(5)	94.3(3)	O(4)−Ni(2)−O(3)	167.3(2)
O(4)−Ni(2)−N(3)	96.7(3)	O(3)−Ni(2)−N(3)	94.5(3)
O(4)−Ni(2)−O(2)	92.7(2)	O(3)−Ni(2)−O(2)	79.0(2)
N(3)−Ni(2)−O(2)	102.6(3)	O(4)−Ni(2)−N(4)	91.4(3)
O(3)−Ni(2)−N(4)	95.5(3)	N(3)−Ni(2)−N(4)	85.0(3)
O(2)−Ni(2)−N(4)	170.8(3)	O(4)−Ni(2)−O(5)	92.6(3)
O(3)−Ni(2)−O(5)	76.1(3)	N(3)−Ni(2)−O(5)	170.6(3)
O(2)−Ni(2)−O(5)	76.1(2)	N(4)−Ni(2)−O(5)	95.5(3)
O(7)−Ni(3)−O(6)	165.1(2)	O(7)−Ni(3)−N(5)	96.4(3)
O(6)−Ni(3)−N(5)	94.7(3)	O(7)−Ni(3)−O(6)#1	89.7(2)
O(6)−Ni(3)−O(6)#1	77.5(3)	N(5)−Ni(3)−O(6)#1	107.2(3)
O(7)−Ni(3)−N(6)	91.7(3)	O(6)−Ni(3)−N(6)	99.4(3)
N(5)−Ni(3)−N(6)	83.4(3)	O(6)#1−Ni(3)−N(6)	169.0(3)
O(7)−Ni(3)−O(8)	93.2(2)	O(6)−Ni(3)−O(8)	76.1(2)
N(5)−Ni(3)−O(8)	170.2(2)	O(6)#1−Ni(3)−O(8)	74.4(2)
N(6)−Ni(3)−O(8)	94.7(2)	Ni(2)−O(5)−Ni(1)	81.0(2)
Ni(1)−O(2)−Ni(2)	91.7(2)	Ni(2)−O(3)−Ni(1)	91.2(3)

[a] Symmetry transformations used to generate equivalent atoms: #1 $-x+1, y, -z+1/2$.

labeling scheme. Bond lengths and angles with estimated standard deviations are given in Table 3.

The structure consists of a $[Ni_2L_2(H_2O)]$ dinuclear species. Each metal atom is coordinated to two nitrogen and two oxygen atoms of a tripodal bis(phenolato) ligand and to an oxygen atom of a similar fragment. The coordination around the nickel atom is completed by an oxygen atom of a water molecule, which acts as a bridge between the two metal atoms. Therefore, both nickel atoms are linked through a triple oxygen bridge, leading to a Ni−Ni distance of 2.9126(15) Å, which is close to those found in other similar dinuclear nickel(II) complexes.[34−36]

The coordination geometry around each nickel atom can be considered as highly distorted octahedral $[NiN_2O_4]$, with the two octahedral polyhedra joined facially through two bridging phenolic oxygens and a water molecule, with the phenolic oxygen atoms of the same ligand in trans positions. The bond angles between the nickel atom and the donor atoms are very different to the expected value of 180° and are in the range 166.8(2)−172.1(3)°. The angles between the nickel atom and the cis donor atoms also differ from 90°, with values in the range 73.7(2)−106.4(3)°. The geometry therefore deviates significantly from the theoretical octahedral arrangement. The apical positions are occupied by the oxygen atom of the bridging water molecule and the secondary amine nitrogen atom located on a pendant arm in the tripodal bis(phenolato) ligand, whereas the equatorial positions are occupied by the other nitrogen atom and the two oxygen atoms of the same ligand and one bridging oxygen atom from the other bis(phenolato) ligand.

Each bridging phenoxy oxygen atom is asymmetrically bound, with one Ni−O bond slightly longer [Ni(1)−O(3) = 2.088(6) Å; Ni(2)−O(2) = 2.076(5) Å] than the other [Ni(1)−O(2) = 1.983(5) Å; Ni(2)−O(3) = 1.987(6) Å]; these latter bond lengths are very similar to those found between the nickel and the terminal phenoxy oxygen atoms [Ni(1)−O(1) = 1.998(5) Å; Ni(2)−O(4) = 1.972(6) Å]. Neither of these distances falls outside the range of average $Ni-O_{phenoxy}$ distances observed in other hexacoordinated nickel(II) complexes [1.971(2)−2.102(7) Å].[37−41]

The bridging water molecule is nearly symmetrically bonded between the two metal atoms [Ni(1)−O(5) = 2.253(7) Å; Ni(2)−O(5) = 2.232(7) Å]. These distances are considerably longer than the other Ni−O distances in the equatorial plane but are within the normal range observed in other similar nickel(II) complexes.[40,42]

Finally, the $Ni-N_{amine}$ bond distances [Ni(1)−N(1) = 2.057(7) Å; Ni(2)−N(3) = 2.053(7) Å] to the pendant arm are shorter than the Ni−N bond lengths [Ni(1)−N(2) = 2.157(7) Å; Ni(2)−N(4) = 2.163(7) Å] of the other amine donor. However, both distances are within the normal range observed in other hexacoordinate nickel(II) complexes of amine ligands [2.048−2.134 Å].[34−37]

The crystal structure of the nickel complex $[Ni_2L_2(H_2O)]\cdot H_2O$ contains water molecules of crystallization, which form hydrogen bonds with the dimeric nickel species (Table 4).

It can be seen in Figure 4 that the dimeric nickel species form groups of three units connected by three water

(34) Nanda, K. K.; Venkatsubramanian, K.; Majundar, D.; Nag, K. *Inorg. Chem*. **1994**, *33*, 1581−1582.
(35) Adams, H.; Clunas, S.; Fenton, D. E. *Inorg. Chem. Commun*. **2001**, *4*, 667−670.
(36) Nanda, K. K.; Das, R.; Thompson, L. K.; Venkatsubramanian, K.; Paul, P.; Nag, K. *Inorg. Chem*. **1994**, *33*, 1188−1193.
(37) Kong, D.; Ouyang, X.; Relbenspies, J.; Clearfield, A.; Martell, A. E. *Inorg. Chem. Commun*. **2002**, *5*, 873−878.
(38) Rybak-Akimova, E. V.; Alcock, N. W.; Busch, D. H. *Inorg. Chem*. **1998**, *37*, 1563−1574.
(39) Luo, H.; Lo, J. M.; Fanwick, P. E.; Stowell, J. G.; Green, M. A. *Inorg. Chem*. **1999**, *38*, 2071−2078.
(40) Mohanta, S.; Namda, K. K.; Werner, R.; Haase, W.; Mukherjee, A. K.; Dutta, S. H.; Nag, K. K. *Inorg. Chem*. **1997**, *36*, 4656−4664.
(41) Mattes, R.; Entian, T. *Z. Anorg. Allg. Chem*. **2003**, *629*, 2298−2304.
(42) F Adams, H.; Clunas, S.; Fenton, D. E. *Chem. Commun*. **2002**, 418−419.

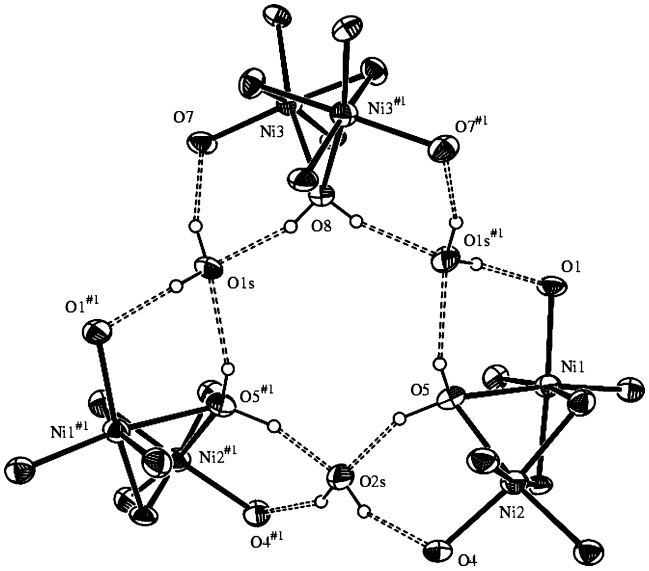

Figure 4. Partial view of the crystal packing for **2.** Dashed lines show the O−H···O interactions.

Table 4. Hydrogen Bond Parameters for **2**

O−H···O	*d*(O−H)	*d*(H···O)	*d*(O···O)	∠(OHO)
O(5)−H(5A)···O(2S)	0.86(2)	1.94(3)	2.758(10)	158(7)
O(5)−H(5B)···O(1S)#1	0.85(2)	1.91(5)	2.728(11)	160(13)
O(8)−H(8)···O(1S)#1	0.85(6)	1.89(6)	2.683(8)	155(6)
O(1S)−H(1SA)···O(7)	0.92(8)	1.77(8)	2.654(9)	159(7)
O(1S)−H(1SB)···O(1)#1	0.86(7)	1.79(7)	2.618(9)	162(7)
O(2S)−H(2S)···O(4)#1	0.82(7)	1.98(8)	2.739(7)	154(9)

molecules. In each of these groups $\{[Ni_2L_2(H_2O)]_3 \cdot 3H_2O\}$ there is a 2-fold rotation axis that passes through the center of O(8) (the bridging water molecule between Ni(3) and Ni(3)#1) and the center of O(2S) (water of crystallization). [Symmetry operation #1: $-x + 1, y, -z + 1/2$]

In these groups, each hydrogen atom of the coordinated water molecules forms a hydrogen bond with a water molecule of crystallization, which in turn is involved in O−H···O interactions with two coordinated water molecules from two neighboring dinuclear units and two nonbridging phenolic oxygens from the same units.

Structure of $[CuL]_2 \cdot 3H_2O$ (3). The molecular structure of **3** is shown in Figure 5 together with the labeling scheme used. Selected bond distances and angles with estimated standard deviations are listed in Table 5.

The structure consists of $[CuL]_2$ dimers that possess a crystallographic 2-fold rotation symmetry that passes through the center of the ring Cu(1)−O(2)−Cu(1)#1−O(2)#2. Each copper atom is coordinated by the two nitrogen and the two oxygen atoms of a ligand. The coordination is completed by an oxygen atom from a similar fragment. The Cu_2O_2 bridge is essentially planar, and none of the atoms deviates from the least-squares plane by more than 0.043 Å. However, the Cu−O bonds are different and the two copper(II) centers are separated by 3.124(3) Å.

The value of 0.6 found for the geometrical parameter τ suggests that the complex has a geometry closer to trigonal-bipyramidal ($\tau = 1$) than to square-pyramidal ($\tau = 0$). The equatorial plane consists of the two phenolate oxygen atoms and the nitrogen atom incorporated as one of the arms of

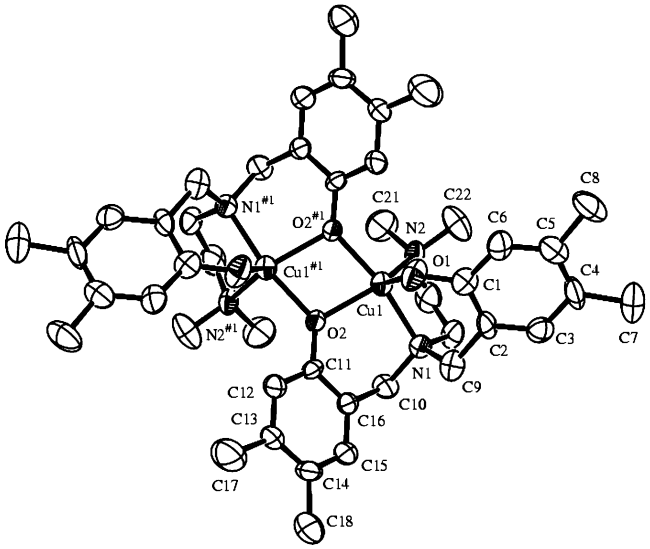

Figure 5. ORTEP diagram of the molecular structure of **3** with 50% thermal ellipsoid probability.

the amine bis(phenolate) ligand. The tripodal nitrogen atom of each ligand and the bridging oxygen atom of a similar fragment are in the apical positions. Each of the two phenolic oxygen atoms that are not involved in the bridge in the two copper centers are arranged in a syn disposition with respect to the Cu_2O_2 core. The copper atom deviates by 0.031 Å from the equatorial plane NO_2.

The angles around the metal atom in the equatorial plane, 130.3(3)−108.3(3)°, are different from the ideal value 120°.

The bond lengths between copper and the phenol oxygen atoms are slightly different [O(2)*−Cu(1) 1.949(5) Å; O(1)−Cu(1) 2.017(7) Å; and O(2)−Cu(1) 2.034(5) Å], with the shorter value corresponding to the apical oxygen atom. These values can be considered as normal and are similar to those found in other pentacoordinate copper(II) complexes that contain bridging phenoxy oxygen atoms [1.929−2.117 Å].[43−46] However, these distances are slightly shorter than one of those found in the dinuclear copper complexes **4**, 2.1816(15) Å (see later) and $[CuL^1]_2$, 2.199(3) Å, where H_2L^1 is *N*,*N*-bis-(2-hydroxybenzyl)-*N*′,*N*′-dimethylethylenediamine—a ligand similar to that used in this study but lacking substituents in the phenyl rings.[47] In these two latter compounds, in contrast to **3**, the two phenolic oxygen atoms are in an anti disposition, which makes the Cu−O−Cu angle in these complexes smaller {99.94(6)° for **4** and 99.7(1)° for $[CuL^1]_2$} and the Cu−Cu distance longer {3.1739(6) Å for **4** and 3.190 Å for $[CuL^1]_2$}.

The $Cu-N_{amine}$ distances are different [Cu(1)−N(1) 2.027(7) Å and Cu(1)−N(2) 2.125(7) Å], with the longer distance corresponding to an apical nitrogen atom. However, both

(43) Bu, X. H.; Du, M.; Zhang, L.; Shang, Z. L.; Zang, R. H.; Shionoya, H. *J. Chem. Soc., Dalton Trans.* **2001**, 729−735.
(44) Vaidyanathan, M.; Palaniandavar, M.; Gopalan, R. S. *Inorg. Chim. Acta* **2001**, *324*, 241−251.
(45) Kong, D. Mao, J.; Martell, A. E.; Clearfield, A. *Inorg. Chim. Acta* **2003**, *342*, 260−266.
(46) Xie, Y.; Liu, Q.; Jiang, H.; Ni, J. *Eur. J. Inorg. Chem.* **2003**, 4010−4016.
(47) Saimiya, H.; Sunatsuki, Y.; Kojima, M.; Tokii, T. *J. Chem. Soc., Dalton Trans.* **2002**, 3737−3742.

Table 5. Selected Bond Lengths (Å) and Angles (deg) for Complexes **3** and **4**

	3[a]	**4**[b]		**3**	**4**
Cu(1)−O(1)	2.017(7)	1.9177(15)	Cu(1)−N(1)	2.027(7)	2.0410(17)
Cu(1)−O(2)	2.034(5)	2.1816(15)	Cu(1)−N(2)	2.125(7)	2.1217(18)
O(1)−C(1)	1.317(10)	1.322(2)	O(2)−C(11)	1.348(8)	1.338(2)
O(2)−Cu(1)#1	1.949(5)	1.9591(14)	Cu(1)−Cu(1)#1	3.124(3)	3.1739/5)
O(1)−Cu(1)−O(2)#1	98.2(3)	94.40(6)	C(11)−O(2)−Cu(1)	122.8(5)	125.39(12)
O(1)−Cu(1)−N(1)	93.7(3)	93.61(7)	Cu(1)#1−O(2)−Cu(1)	103.3(2)	99.94(6)
O(2)#1−Cu(1)−N(1)	166.3(3)	169.25(6)	O(1)−Cu(1)−N(2)	121.3(3)	142.18(8)
O(2)#1−Cu(1)−N(2)	93.3(3)	92.52(7)	N(1)−Cu(1)−N(2)	86.3(3)	85.51(7)
O(1)−Cu(1)−O(2)	108.3(3)	115.43(7)	O(2)#1−Cu(1)−O(2)	76.5(2)	80.06(6)
N(1)−Cu(1)−O(2)	93.3(2)	90.03(6)	N(2)−Cu(1)−O(2)	130.3(3)	102.39(6)

[a] Symmetry transformations used to generate equivalent atoms: #1 $-x+1, y, -z+3/2$. [b] Symmetry transformations used to generate equivalent atoms: #1 $-x+1, -y, -z$.

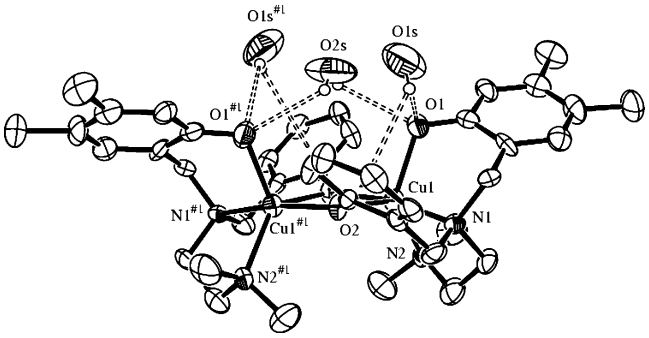

Figure 6. The hydrogen bonding in **3**. Dashed lines show the O−H···O and the O−H···π interactions.

bond lengths are within the normal range for interactions of this type [1.925−2.097 Å].[43−47]

The crystal structure of the copper complex, **3**, contains water molecules of crystallization that form hydrogen bonds with the dimeric copper units (Figure 6). One difference between this complex and the nickel analogue is that the three water molecules do not connect different adjacent dimeric copper units but interact with only one dimeric unit.

Each dimeric unit has a 2-fold axis of rotation that passes through the center of the Cu_2O_2 group [symmetry operation #1: $-x+1, y, -z+3/2$].

The water molecule contained in the axis, O(2S), is very loosely associated and is involved in a weak interaction with the other water molecules of crystallization O(1S) and O(1S)-#1 as an acceptor of O−H···O interactions and with the phenolic oxygens that are not involved in the Cu_2O_2 bridge as a donor in O−H···O interactions. The interactions involving the molecule in the axis, O(S), are only slightly directional, as observed from the OHO angles in Table 6.

The water molecule of crystallization O(1S) is involved in interactions with one of the ligands in the dimer, and the other water molecule, O(1S)#1, is involved in an equivalent interaction with the equivalent ligand in the dimer—given that they are related through the 2-fold rotation axis. These water molecules, O(1S) and O(1S)#1, are involved in two types of interaction: (a) a hydrogen-bonding interaction O−H···O, O(1S)−H(2S)···O(1) where O(1) is the phenolic oxygen that is not involved in the bridge and (b) an O−H···π interaction, O(1S)−H(1S)···ct, where ct signifies the centroid of the phenolic ring of the ligand that contains the bridging oxygen, denoted as C(11)−C(16) [d(O(1S)−ct) = 3.374 Å, d(H(1S)−ct) = 2.694 Å, ∠(O(1S)−H(1S)−ct) = 139.57°].

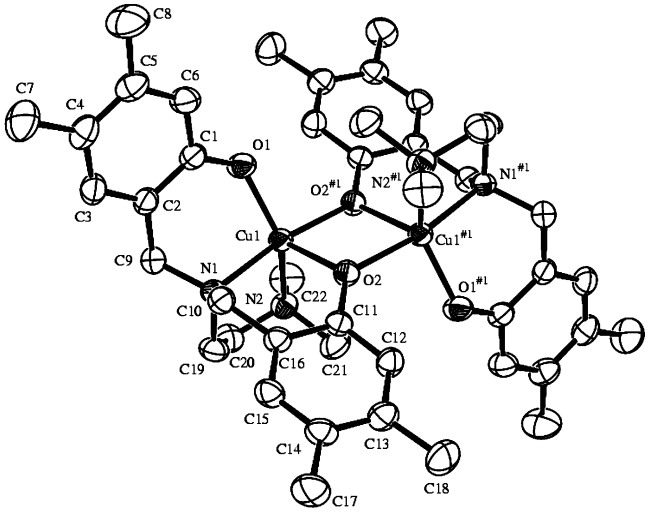

Figure 7. ORTEP diagram of the molecular structure of **4** with 50% thermal ellipsoid probability.

Table 6. Hydrogen Bond Parameters for **3**

O−H···O	d(O−H)	d(H···O)	d(O···O)	∠(OHO)
O(1S)−H(2S)···O(1)	0.84(2)	2.77(4)	3.60(2)	171(13)
O(1S)−H(2S)···O(2S)	0.84(2)	2.51(14)	3.042(17)	122(14)
O(2S)−H(3S)···O(1)	0.78(10)	2.31(10)	2.732(11)	115(9)

Structure of $[CuL]_2 \cdot 2CH_3CN$ (4). The product obtained in the electrochemical synthesis of the Cu(II) complex with H_2L and 1,10-phenanthroline was found to be **4**, a geometric isomer of **3**. The phen coligand was not incorporated into the coordination sphere of the metal.

The molecular structure of this complex is shown in Figure 7 along with the atom numbering scheme. Selected bond distances and angles are given in Table 5.

The complex presents a dimeric structure that has a crystallographic inversion center in the unit cell. Each copper atom has a CuO_3N_2 pentacoordinated environment and is bonded by two anionic ligands than act as bridges between the two metal atoms in a similar way to that found in **3**. However, the coordination geometry in **4** is different to that described above for **3**. In this case, the geometry, ($\tau = 0.45$) is closer to square-pyramidal ($\tau = 0$) than to trigonal-bipyramidal ($\tau = 1$). Moreover, the disposition of the ligand is such than the apical tripodal nitrogen atoms are in an anti disposition, whereas in **3** they are in a syn disposition. As

in **3**, both copper atoms in complex **4** are linked through a double phenoxy oxygen bridge, leading in this case to a Cu−O−Cu bridge angle [99.94(6)°] that is lower than that found in **3**, 103.3(2)°, and a Cu···Cu distance [3.1739(6)Å] longer than that in **3**, 3.124(3) Å.

The Cu−N distances, 2.1217(18) and 2.0410(17) Å, are similar to those found in **3**. However, the Cu−O nonbridging distance is shorter, 1.9177(15) Å, and one of the Cu−O bridging distances is greater, 2.1816(15) Å, than the corresponding distances in **3** [2.017(7) and 2.034(5) Å, respectively]

The compound crystallizes with two acetonitrile molecules, which do not interact with the copper complex in any significant manner, and noteworthy intermolecular contacts are not observed.

IR Spectroscopy and Mass Spectrometry. In all cases, the bands in the free ligand at 3350−3100 cm^{-1}, attributable to O−H stretching of phenol groups with weak intramolecular hydrogen bonding, are absent in the spectra of the corresponding complexes. In addition, the band attributable to ν(CO), which in the free ligand appears at 1294 cm^{-1}, is shifted to higher wavenumbers (1314−1307 cm^{-1}) in the complexes. The δ(OH) band of the phenol hydroxy group, which is observed in the ligand at 1235 cm^{-1}, is not observed in the complexes. These results show that the phenol hydrogen atoms are lost during the electrochemical synthesis and that the ligand is dianionically coordinated to the metal ions through both phenol oxygen atoms. Moreover, it has been claimed that the splitting of the ν(CO) band into four components in the range 1200−1100 cm^{-1} is characteristic of bridging phenol oxygen atoms in both homo- and heteronuclear complexes.[48] However, in our case the ligand presents a large number of bands in this range, making it difficult to identify which bands are due to the complexes. Therefore, it is impossible to conclude whether the rule is applicable to complexes **1**−**4** or not.

The electrospray mass spectra show the peaks associated with the dimeric units $[M_2L_2]^+$ and these have the appropriate isotope distribution (m/z = 826, 844, and 836, respectively, for M = Co, Ni, and Cu). A peak associated with $[M_2L]$ fragments formed by loss of the amine bis(phenolate) ligand from the initial dimeric species is also observed in each case (m/z = 472, 473, and 481, respectively, for M = Co, Ni, and Cu). In the nickel complex, the peak for the $[Ni_2L_2 - H_2O]$ fragment formed by loss of a water molecule from the dimeric unit is also observed at m/z = 826. In addition, in all cases peaks due to the monomeric unit [ML] are observed at m/z = 413, 413, and 418 (for M = Co, Ni, and Cu) and the free ligand at m/z = 354.

UV Spectroscopy. The diffuse reflectance spectrum of the cobalt complex shows the characteristic features of five-coordinated cobalt(II) ions with a distorted trigonal bipyramidal stereochemistry.[49] It is difficult to unequivocally assign the bands observed to specific electronic transitions, but according to the energy level diagram for cobalt(II) in a trigonal bipyramidal field, the bands in the visible region at about 13500 and 18600 cm^{-1} are assigned to $^4A_2'(F) \rightarrow {}^4E'(F)$ and $^4A_2'(F) \rightarrow {}^4E''(P)$ transitions, respectively. The broad band in the near-IR region at about 6000 cm^{-1} is assigned to $^4A_2'(F) \rightarrow {}^4E''(F)$ and the shoulder at 11 600 cm^{-1} to $^4A_2'(F) \rightarrow {}^2E'(G)$ transitions.

The nickel(II) complex was also studied by electronic spectroscopy in the solid state. The compound shows a very broad band at around 9540 cm^{-1} with a shoulder at 7800 cm^{-1} and two further bands at 15800 and 22300 cm^{-1}. These absorptions are within the accepted range for hexacoordinated octahedral nickel(II) complexes and can be assigned to the transitions $^3A_{2g} \rightarrow {}^3T_{2g}$ (ν_1), $^3A_{2g} \rightarrow {}^3T_{1g}(F)$ (ν_2), and $^3A_{2g} \rightarrow {}^3T_{1g}(P)$ (ν_3), respectively.[49] The shoulder at 7800 cm^{-1} can be attributed to band splitting as a consequence of the distortion of octahedral symmetry.

The solid-state reflectance spectra of copper(II) complexes display two bands; one broad band at 8900 cm^{-1} for **3** and 9090 cm^{-1} for **4** and other at 22 600 cm^{-1} for **3** and 21 740 cm^{-1} for **4**. These features are consistent with a geometry intermediate between trigonal bipyramidal and square pyramidal around copper(II).[49]

Magnetic Properties. The magnetic behavior of the dinuclear complex **3** expressed in the form of χ_M versus T, where χ_M is the molar magnetic susceptibility and T the temperature, is shown in Figure 8. In the temperature range 300−250 K, χ_M has a value close to 1.55×10^{-3} cm^3 mol^{-1}, which is significantly lower than the value expected for two magnetically uncoupled Cu(II) ions ($2.50\ 10^{-3}$ cm^3 mol^{-1} for $g = 2$). At temperatures below 250 K, χ_M decreases continuously to reach a minimum of ca. 5.80×10^{-4} cm^3 mol^{-1} at 75 K. The value then increases again as the temperature is lowered further. This behavior is typical for compounds that display strong intramolecular antiferromagnetic coupling. The increase in χ_M at low temperatures corresponds to impurities, usually attributed to monomeric Cu(II) species. To confirm this hypothesis, we analyzed the magnetic data through the spin-only formalism including the Zeeman perturbation (eq 1):

$$\hat{H} = -J\hat{S}_A\hat{S}_B + \beta g\hat{S}_A H \qquad (1)$$

implying an isotropic Heisenberg interaction with $S_A = S_B = 1/2$. The resulting χ_M versus T expression deduced from eq 1 is the so-called Bleaney−Bowers expression, which was implemented to account for of the paramagnetic impurities. The parameters J, g, and β have their usual meanings. The parameters J, g, and ρ (percentage of paramagnetic impurities) were determined by minimizing the least-squares fit. The best fit for calculated and experimental χ_M values was found for $J = -327$ cm^{-1}, $g = 2.11$, $\rho = 0.07$, and $R = 1.8 \times 10^{-4}$ for **3** and $J = -45$ cm^{-1}, $g = 2.17$, $\rho = 0.048$, and $R = 3 \times 10^{-4}$ for **4**. R is the agreement factor defined as $\Sigma_i[(\chi_M)_i^{exptl} - [(\chi_M)_i^{calcd}]^2/[(\chi_M)_i^{exptl}]^2$. Temperature-independent paramagnetism (TIP) was considered equal to 120×10^{-6} cm^3 mol^{-1}. The solid lines in Figures 8 and 9 correspond to the calculated curves, and these show excellent agreement

(48) Samus, N. M.; Strelkov, E. A.; Tsapkov, V. I.; Gulya, A. P. *Russ. J. Coord. Chem.*, **2004**, *30*, 275−279 and references therein.
(49) Lever, A. B. P. *Inorganic Electronic Spectroscopy*, 2nd ed.; Elsevier: Amsterdam, 1984.

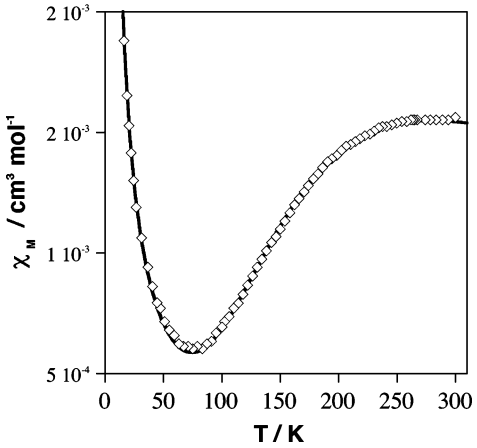

Figure 8. χ_M versus T plot for compound **3**. The solid line represents the best fit to the experimental data (see text).

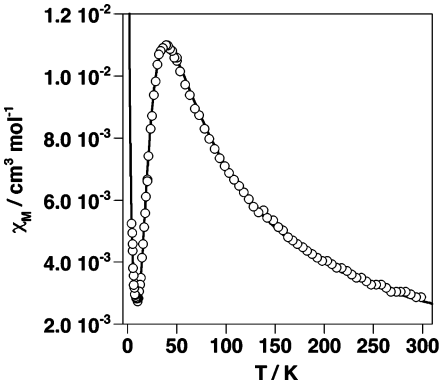

Figure 9. χ_M versus T plot for compound **4**. The solid line represents the best fit to the experimental data (see text).

between the experimental and theoretical χ_M data. The magnitude and sign of J, determined by the angle 103.3(2)° defined by Cu−O−Cu, confirms the strong antiferromagnetic interaction operating through the double phenoxo group bridge in **3**. However, this value is lower than one would expect from theoretical calculations and lower than that that observed in related hydroxo- and alkoxo-bridged binuclear copper complexes.[50] The absolute value of J is essentially mitigated by the strong distortion observed in the coordination geometry of the Cu(II) ion, which lies between a square-pyramidal and trigonal bipyramidal [CuN_2O_3] core ($\tau \approx \pi 0.6$). This situation leads to a distribution in the spin density between the d_{xy}-type and the d_{z^2} orbitals and decreases the magnitude of the magnetic coupling. Compound **4** has Cu−O−Cu angles of 99.94(6)°, and consequently, the magnitude of J is much smaller than that of **3**. Compounds **3** and **4** are closely related to [$Cu_2L^1{}_2$], where L^1 is the deprotonated form of *N*,*N*-bis(2-hydroxybenzyl)-*N*′,*N*′-dimethylenediamine.[47] The latter complex displays a very weak magnetic coupling, $J = -19.9$ cm^{-1}, as its coordination core is distorted in a similar way to **4** and the Cu−O−Cu angle is 99.7(1)°.

The magnetic behavior of **2** is represented in Figure 10 as a plot of $\chi_M T$ product versus T. $\chi_M T$ is equal to 2.58 cm^3 K mol^{-1} at 275 K, a value higher than that expected for the

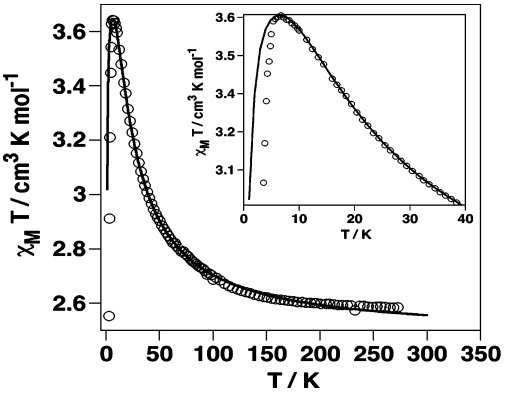

Figure 10. $\chi_M T$ versus T plot for compound **2**. The solid line represents the best fit to the experimental data (see text).

contribution of two $S = 1$ spin centers without considering the orbital contribution ($g = 2$). On cooling, $\chi_M T$ increases to reach a maximum (3.65 cm^3 K mol^{-1}) at around 6.8 K, a value that corresponds well with an $S = 2$ ground state stemming from the occurrence of ferromagnetic coupling between the two $S = 1$ centers. Below this temperature, $\chi_M T$ drops rapidly to a value of 1.72 cm^3 K mol^{-1} at 1.8 K. This behavior could be associated with the occurrence of zero-field splitting and/or intermolecular antiferromagnetic interactions. Consequently, the following Hamiltonian (eq 2) was used to analyze the experimental data:

$$\hat{H} = -J\hat{S}_A\hat{S}_B + D(\hat{S}_A^2 + \hat{S}_B^2) + \beta g\hat{S}_A H \qquad (2)$$

where D corresponds to the zero-field splitting parameter and $S_A = S_B = 1$. The susceptibility equation is taken from the literature.[51] The best fit for calculated and experimental data was achieved for $J = 9.9$ cm^{-1}, $D = 3.1$ cm^{-1}, $g = 2.22$, and $R = 1 \times 10^{-5}$, which corresponds to the solid line in Figure 10. It is worth noting that for temperatures below 6 K the experimental $\chi_M T$ values drop much faster than the calculated ones (see inset in Figure 10). This fact, which cannot be accounted for by introducing antiferromagnetic intermolecular interactions into the model, could stem from magnetic ordering. A plot of the experimental magnetization (M) versus the magnetic field (H) at 2 K is shown in Figure 11 together with the calculated values using the D and g values deduced above (solid line). All these data confirm the occurrence of a ferromagnetic interaction and a fundamental state, $S = 2$, for the molecule. The triple bridge formed by the oxygen atoms of two phenoxo groups and a molecule of water define angles of 91.7(2)°, 91.2(3)°, and 81.0(2)°, respectively. This situation favors ferromagnetic exchange through the accidental orthogonality of the orbitals with the unpaired electrons (magnetic orbitals).[52]

The magnetic properties of compound **1** expressed in the form of $\chi_M T$ and χ_M versus T are depicted in Figure 12. The susceptibility curve shows a rounded maximum at 14 K (0.114 cm^3 mol^{-1}), whereas $\chi_M T$ exhibits a continuous decrease upon cooling to give $\chi_M T = 4.70$ cm^3 K mol^{-1} at

(50) Ruiz, E.; Alemany, P.; Álvarez, S.; Cano, J. *J. Am. Chem. Soc.* **1997**, *119*, 1297−1303 and references herein.

(51) Ginsberg, A. P.; Martin, R. L.; Brookes, R. W.; Sherwood, R. C. *Inorg. Chem.* **1972**, *11*, 2884−2889.

(52) Kahn, O. *Molecular Magnetism*; VCH: New York, 1993.

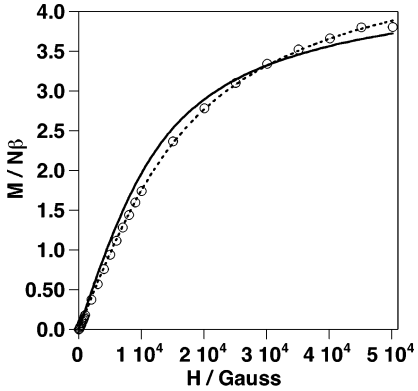

Figure 11. Experimental magnetization (M) versus magnetic field (H) (circles) and calculated for $D = 3.1$ cm^{-1} and $g = 2.22$ (solid line) plots at 2 K for compound **2**.

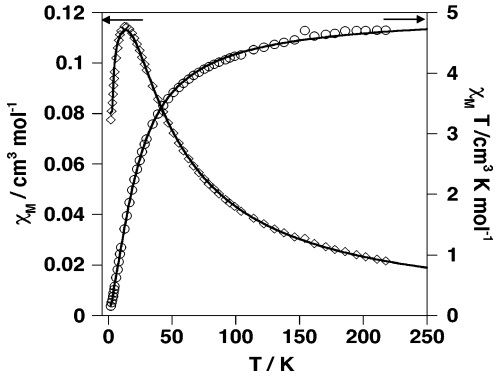

Figure 12. $\chi_M T$ (right) and χ_M (left) versus T plots for compound **1**. The solid lines correspond to the best fit.

220 K. This is a reasonable value for two high-spin cobalt(II) ions with strong orbital contributions. The extrapolated value of $\chi_M T$ vanishes as T approaches zero. Such behavior is characteristic of an intramolecular antiferromagnetic interaction. The experimental data were reproduced satisfactorily using the formalism described above for compound **3** but considering that $S_A = S_B = 3/2$. The best fit between calculated and experimental data corresponds to $J = -7.5$ cm^{-1}, $g = 2.29$, $\rho = 0.028$, TIP $= 113 \times 10^{-6}$, and $R = 2 \times 10^{-4}$.

The fact that compounds **1** and **3** exhibit negative J values is consistent with their structural similarity at the molecular level. The bond distances and angles are very similar, with the most relevant difference corresponding to the bridge angle Co−O−Co of 102.04(7)°, which is 1.26° smaller than that in compound **3**. However, it is important to point out that comparison between the magnitude of the magnetic coupling of Cu(II) and Co(II) derivatives cannot be made from direct comparison of the J values as the Co(II) ion has two additional unpaired electrons. In this case, the J value is the sum of the individual contributions, J_{ij}, involving each pair of magnetic orbitals involved in the exchange phenomenon (eq 3):

$$J = \frac{1}{n^2}\sum_{i,j}^{n} J_{ij} \tag{3}$$

where n is the number of unpaired electrons of the metal center. According to this equation, the net antiferromagnetic interaction is defined by n^2J.[52] Consequently, it is expected that J[Cu(II)] $\approx n^2J$[Co(II)]. In the present case, n^2J[Co(II)] is -67.6 cm^{-1}—a value four times smaller than that obtained for the binuclear Cu(II) compound **3**. This marked difference can be ascribed to the significantly smaller Co−O−Co angle.

Conclusion. The potentially dianionic tetradentate Mannich base ligand H_2L stabilizes neutral dinuclear complexes of Co(II), Ni(II), and Cu(II) formed by an electrochemical method. This synthetic procedure allowed us to obtain neutral complexes of the type $[ML]_2$ with high purity and in very good yield.

Despite the title complexes being dimers that are formed with identical ligands, their structures show considerable variation. The X-ray structure of the nickel(II) complex shows that the nickel(II) ions are hexacoordinate in distorted octahedral environments with both Ni(II) ions bonded through three oxygen bridges; these bridges favor ferromagnetic coupling between the Ni(II) ions. In the case of Co(II), the ligand forms a phenoxo-bridged binuclear complex in which each cobalt is in a trigonal-bipyramidal environment. The magnetic moment for the cobalt compound shows that both Co(II) atoms are antiferromagnetically coupled. In the case of Cu(II), two different dinuclear compounds with two phenoxy group bridges are obtained. The reason for the differences in the structures of complexes **3** and **4** are probably due to the presence of water molecules of crystallization in **3**. These water molecules in **3** are involved in several O−H···O intramolecular hydrogen bonds with the two nonbridging phenol oxygen atoms. This leads to a situation where these two phenolic oxygen atoms are in a syn disposition and the geometry around each copper atom

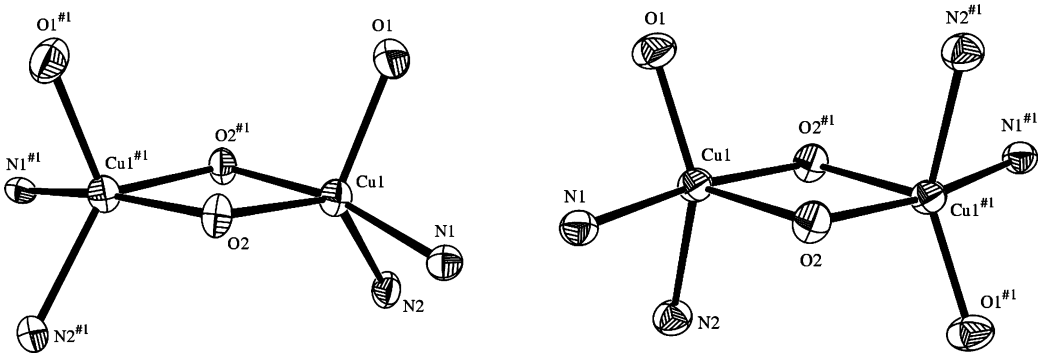

Figure 13. A view of the coordination sphere of the metals in **3** (left) and in **4** (right).

is closer to trigonal bipyramidal, with a Cu−O−Cu angle of 103.3(2)°. The absence of water molecules in **4** leads to a structural difference compared to **3** in that the nonbridging phenolic oxygen atoms are in an anti disposition (Figure 13) and the coordination geometry for **4** is closer to square pyramidal, with a Cu−O−Cu angle of 99.94(6)°. The magnetic moments for these two compounds are quite different; the values indicate a strong antiferromagntic coupling of the Cu(II) ions ($2J = -654$ cm^{-1}) for **3** and weak antiferromagnetic coupling for **4**. These values are consistent with the known correlation between the Cu−O−Cu bridging angle and the sign of magnetic coupling constant J in Cu(II) dinuclear complexes.

Acknowledgment. This work was supported by Xunta de Galicia (Spain) (Grant No. PGIDT00PXI20305PR) and by the Ministerio de Ciencia y Tecnología (Spain) (Grant No. BQU2002-01819).

Supporting Information Available: Crystallographic data in cif format. This material is available free of charge via the Internet at http://pubs.acs.org.

IC0602594